Journal of Applied Fluid Mechanics, Vol. 11, No. 4, pp. 995-1004, 2018.
Available online at www.jafmonline.net, ISSN 1735-3572, EISSN 1735-3645.
DOI: 10.29252/jafm.11.04.27870

Drag Experienced by a Composite Sphere in an Axisymmetric Creeping Flow of Micropolar Fluid

V. Mishra and B. R. Gupta

Department of Mathematics, Jaypee University of Engineering & Technology, Guna, M. P., India

†*Corresponding Author Email: baliram.gupta@juet.ac.in*

(Received April 14, 2017; accepted January 13, 2018)

ABSTRACT

This paper concerns an analytical study of a steady axisymmetric uniform flow of an incompressible micropolar fluid past a permeable sphere that contains a solid sphere. The mathematical expression for the flow fields are obtained in terms of stream function by using modified Bessel's function and Gegenbauer function. No-slip condition, zero microrotation components, continuity of normal velocity which is equal to the filtration velocity on the surface of the sphere are used as boundary conditions. It is assumed that the fluid obeys Darcy law at the permeable surface. The internal and external drag force exerted by the fluid on the sphere, flow rate and the relevant quantities such as pressures, microrotation vectors have been calculated. It is observed that drag is greater for impermeable sphere as compared to permeable sphere. As permeability parameter increases the flow rate also increases rapidly. Various useful results are obtained and compared with the previous particular cases.

Keywords: Permeable sphere; Micropolar fluid; Drag force; Stream function; Darcy law.

NOMENCLATURE

a	radius of the permeable sphere	υ_ϕ	micro-rotation component
b	radius of the solid sphere	ψ	stream function
$\bar{\mathrm{v}}$	velocity vector	D	drag force
μ	dynamic viscosity	D_N	dimensionless drag
κ	vertex viscosity	$G_N(\zeta)\,\&\,H_N(\zeta)$	Gigenbauer functions
ω	microrotation vector	$K_{3/}(\lambda r)\,\&\,I_{3/}(\lambda r)$	modified Bessel functions
α,β,γ	gyro viscosity coefficients	T	stress tensor
p	pressure	Q	rate of flow

1. INTRODUCTION

Since recent past the flow through permeable media has been a longstanding topic for researchers due to its numerous applications in various fields like geophysical and biomechanical problems etc. Also it is most applicable in the field of chemical engineering. For example when examining the hindered settling flocs. The most practical example of physical process of viscous flow with in permeable spherical region is the structure of earth. Darcy (1856) initially proposed the equation of motion for fluid flow in permeable medium with low porosity systems, such as sand, beds, sintered materials and petroleum reservoir rocks etc. Leonov (1962) has solved the problem of the slow stationary flow of a viscous fluid about a permeable sphere by taking the small thickness of the permeable surface and determined the resistance exerted by the fluid on the sphere. Wolfersdorf (1989) solved the problem of creeping flow past a permeable sphere and additionally past a permeable sphere containing concentric impermeable sphere for the Newtonian fluid by using the Darcy law and

no-slip condition at the surface of the sphere and obtained that drag on permeable sphere is less than that of rigid sphere. Birikh and Rudakoh (1982) solved the problem of slow motion of a permeable sphere in viscous fluid and evaluated the drag and flow rate. Padmavati *et al*. (1995) solved the problem of Stokes flow past a sphere with permeable surface for non-axisymmetric case and gave a general method for calculating non-axisymmetric flow both outside and inside the permeable spherical boundary and found the expression for the drag and torque on the sphere using representation for the pressure and velocity following Palaniappan *et al*. (1990). The problem of laminar flow past a permeable sphere solved by Nandakumar and Masliyah (1982) by using Navier Stokes equation outside the sphere and Brinkman's equation inside the sphere and observed that the computed drag factors are 10% less than the experimental value observed by Malsiyah and Polikar (1980). Usha R. (1995) solved the problem of Stokes flow with concentric permeable spheres in relative motion. Slow viscous fluid past a spinning sphere with permeable surface studied by Vasudeviah and Malathi (1995) and they derived the expression for the drag coefficient on the body which can be used as formula for the determination of the permeability of the sphere. Murthy *et al*. (2007) in an earnest attempt, studied the problem of uniform flow of an incompressible couple stress fluid past a permeable sphere.

The mathematical model of micropolar fluid enables us to study many physical phenomena arising from the local structure and micro-motions of the fluid particles. It describes the behavior of numerous real fluids such as polymeric suspensions, liquid crystals, muddy fluids, and animal blood. The theory of micropolar fluid was introduced by Eringen (1966). Drag on axially symmetric body in the Stokes flow of micropolar fluids was studied by Ramkissoon and Majumdar (1976) and they derived the general expression for the drag of an axially symmetric body in Stokes flow. Rao and Rao (1970), Rao and Iyengar (1981) and Iyengar and Srinivasacharya (1993) considered the problem of Micropolar fluid past a rigid sphere, spheroid and approximate sphere respectively. Creeping flow of micropolar fluid past a porous sphere was solved by Srinivasacharya and Rajyalaxmi (2004); they observed that the drag in micropolar fluid is more than that of Newtonian fluid. E.I. Saad (2012) studied cell models for micropolar flow past a viscous fluid sphere using Happel, Kuwabara, Kanningham and Kvashnin cell models and obtained the drag force acting on the sphere. Uniform flow of an incompressible micropolar fluid past a permeable sphere is considered by Aparna and Murthy (2010); they also studied (2015, 2016) the problem on slow steady rotation of a permeable sphere with thin surface in an incompressible couple stress fluid and noticed that due to internal flow, couple acting on the sphere is zero.

In recent years, the applications of compound multiphase drops, which are made of an outer permeable or liquid shell and an inner rigid sphere, gas bubble or immiscible liquid drop, have received significant interest. Axisymmetric creeping flow of a micropolar fluid over a sphere coated with a thin fluid film studied by Gupta and Deo (2013) using the modified Bessel's function and Gigenbaur function concluded that a sphere without coating experiences greater resistance in comparison to coated fluid. The slow steady rotation of micropolar fluid sphere in concentric spherical container using non-zero boundary condition for microrotation vector was solved by Madasu and Gurdatta (2015) and they obtained the hydrodynamic couple and wall correction factor exerted on the micropolar fluid. Mishra and Gupta (2016) solved the problem of drag on permeable sphere placed in micropolar fluid with non-zero boundary condition for micro-rotation and they observed that drag is greater in the case of zero micro-rotation vector than in the case of non-zero micro-rotation vector. Later on they (2017) also considered the problem of motion of a permeable shell in a spherical container filled with micropolar fluid.

This study undertakes the problem of steady axisymmetric creeping flow of a micropolar fluid past a permeable sphere that contains a solid sphere. It is further assumed that the motion is sufficiently slow. The explicit expressions of the flow fields are obtained by using different boundary conditions satisfying at the surface of the sphere like conjugacy condition of Darcy type, zero microrotation vector, no-slip condition, uniform velocity at infinity etc. It is observed that drag force increases as the inner solid sphere expands. Drag is greater for the impermeable sphere.

2. MATHEMATICAL FORMULATION OF THE PROBLEM

Consider a permeable sphere of radius a that contains a rigid sphere of radius b $(a > b)$ in an unbounded medium with origin at the centre O of the sphere (Fig. 1). It is assumed that the composite sphere is stationary and a steady axisymmetric Stokes flow of micropolar fluid has been established around it by a uniform far-field flow with velocity of magnitude U directed along Z-axis. The thickness of permeable sphere is assumed very small in comparison the radius a and b.

Under the Stokes approximation in the absence of body force and body couple the general form of governing equations for the slow steady motion of micropolar fluids can be written as

$$\nabla.\bar{\mathrm{v}} = 0, \tag{1}$$

$$-\nabla \mathrm{p} + \kappa \nabla \times \bar{\omega} - (\mu + \kappa)\nabla \times (\nabla \times \bar{\mathrm{v}}) = 0, \tag{2}$$

$$-2\kappa\bar{\omega} + \kappa\nabla \times \bar{\mathrm{v}} - \gamma\nabla \times (\nabla \times \bar{\omega}) + (\alpha + \beta + \gamma)\nabla(\nabla.\bar{\omega}) = 0, \tag{3}$$

where $\bar{\mathrm{v}}$, p, $\bar{\omega} = \upsilon_\phi(r,\theta)\hat{e}_\phi$ are the velocity vector, pressure, microrotation vector, μ is the classical viscosity coefficient of the fluids, κ is the

vortex viscosity coefficients and α,β,γ are the gyro viscosity coefficients satisfying the following inequalities

$$3\alpha+\beta+\gamma=0,\ \ 2\mu+\kappa\geq 0,\ \ \gamma\geq|\beta|,\ \ \kappa\geq 0,\ \ \gamma\geq 0. \tag{4}$$

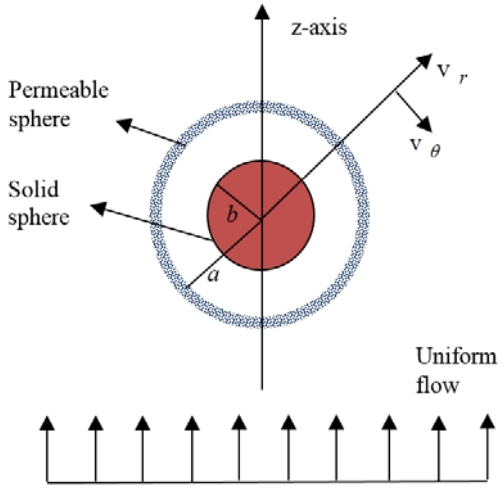

Fig. 1. Flow diagram.

Since all the flow functions are independent of ϕ for the axially symmetric flow field, therefore we can introduce stream functions $\psi(r,\theta)$ which is related to the velocity in spherical coordinate system (r,θ,ϕ) by Happel and Brenner (1983)

$$\bar{\mathrm{v}}=\mathrm{v}_r(r,\theta)\hat{e}_r+\mathrm{v}_\theta(r,\theta)\hat{e}_\theta=-\mathrm{curl}\left[\frac{\psi}{r\sin\theta}\hat{e}_\phi\right], \tag{5}$$

and we find two velocity components of the flow as

$$\mathrm{v}_r=-\frac{1}{r^2\sin\theta}\frac{\partial\psi}{\partial\theta},\ \ \mathrm{v}_\theta=\frac{1}{r\sin\theta}\frac{\partial\psi}{\partial r}. \tag{6}$$

From (5) and (6) we have

$$\nabla\times\bar{\mathrm{v}}=\frac{E^2\psi}{r\sin\theta}e_\phi\ \ \nabla\times\nabla\times\nabla\times\bar{\mathrm{v}}=\frac{-E^4\psi}{r\sin\theta}e_\phi \tag{7}$$

and we also find

$$\nabla\times\nabla\times\bar{\omega}=\frac{-E^2(r\sin\theta\upsilon_\phi)}{r\sin\theta}e_\phi \tag{8}$$

In order to non-dimensionalize the equations and variables, we put

$$r=a\tilde{r}\ \ \psi=Ua^2\tilde{\psi},\ \ \mathrm{p}=\frac{\mu U}{a}\tilde{\mathrm{p}},\ \ \upsilon_\phi=\frac{U}{a}\tilde{\upsilon}_\phi$$

and dropping tildes subsequently in further analysis. Substituting the value of Eqs. (7) and (8) in Eq. (3) we obtain

$$E^2\left(r\sin\theta\upsilon_\phi\right)=\frac{2\kappa}{\gamma}r\sin\theta\upsilon_\phi-\frac{\kappa}{\gamma}E^2\psi. \tag{9}$$

Taking curl of Eq. (2) and using Eqs. (7) and (8) we obtain

$$-\kappa E^2\left(r\sin\theta\upsilon_\phi\right)+(\mu+\kappa)E^4\psi=0. \tag{10}$$

From Eqs. (9) and (10) we have

$$\upsilon_\phi=\frac{1}{2r\sin\theta}\left\{E^2\psi+\frac{\gamma(\mu+\kappa)}{\kappa^2}E^4\psi\right\}. \tag{11}$$

Eliminating the pressure from Eq. (2) and using Eq. (3) we get the differential equation

$$E^4\left(E^2-\lambda^2\right)\psi=0, \tag{12}$$

where $E^2=\frac{\partial^2}{\partial r^2}+\frac{\left(1-\zeta^2\right)}{r^2}\frac{\partial^2}{\partial\zeta^2}$, $\zeta=\cos\theta$ and micropolar parameter

$$\lambda^2=\frac{\kappa(2\mu+\kappa)a^2}{\gamma(\mu+\kappa)}. \tag{13}$$

The constitutive equation for isotropic non-Newtonian micropolar fluid is given by (1966 Eringer)

$$T_{ij}=\left(-\mathrm{p}+\mu div\bar{\mathrm{v}}\right)\delta_{ij}+(2\mu+\kappa)d_{ij}+\kappa\varepsilon_{ijm}\left(\xi_m-\omega_m\right), \tag{14}$$

where, $d_{ij}=\frac{1}{2}\left(\mathrm{v}_{i,j}+\mathrm{v}_{j,i}\right)$ is the rate of strain, T_{ij} is the stress tensor, δ_{ij} is the kronecker delta, ξ_m is the vorticity vector, ω_m is the component of microrotation vector.

The expression of normal and tangential stresses in axisymmetric spherical coordinate are obtained using Eq. (14) and given by

$$T_{rr}=-\mathrm{p}+\frac{(2\mu+\kappa)}{r^2\sin\theta}\left(\frac{2}{r}\frac{\partial\psi}{\partial\theta}-\frac{\partial^2\psi}{\partial r\partial\theta}\right), \tag{15}$$

$$T_{r\theta}=\frac{(2\mu+\kappa)}{2r^2\sin\theta}\left(r\frac{\partial^2\psi}{\partial r^2}-2\frac{\partial\psi}{\partial r}-\frac{1}{r}\frac{\partial^2\psi}{\partial\theta^2}+\frac{\cot\theta}{r}\frac{\partial\psi}{\partial\theta}\right)+k\left(\xi_m-\omega_m\right). \tag{16}$$

3. SOLUTION OF THE PROBLEM

The solution of Eq. (12) can be obtained by superimposing the solution of

$$E^2\psi_0=0,\ \ E^4\psi_1=0,\ \ \left(E^2-\lambda^2\right)\psi_2=0, \tag{17}$$

in the form

$$\psi=\psi_0+\psi_1+\psi_2. \tag{18}$$

Using method of separation of variable in Eq. (17) we get the values of ψ_0, ψ_1, ψ_2 and from Eq. (18) we get the general solution of Eq. (12) as

$$\psi = \sum_{n=0}^{\infty} \Big\{ \Big[A_n' r^n + B_n' r^{-n+1} + C_n' r^{n+2} + D_n' r^{-n+3} + E_n' \sqrt{r} K_{n-\frac{1}{2}}(\lambda r) + F_n' \sqrt{r} I_{n-\frac{1}{2}}(\lambda r) \Big] G_n(\zeta) + \Big[A_n r^n + B_n r^{-n+1} + C_n r^{n+2} + D_n r^{-n+3} + E_n \sqrt{r} \times K_{n-\frac{1}{2}}(\lambda r) + F_n \sqrt{r} I_{n-\frac{1}{2}}(\lambda r) \Big] H_n(\zeta) \Big\} \quad (19)$$

Here $K_{n-\frac{1}{2}}(\lambda r)$, $I_{n-\frac{1}{2}}(\lambda r)$ are modified Bessel functions and $G_n(\zeta)$, $H_n(\zeta)$ are Gigenbaur function of first and second kinds respectively.

We have ignored the terms which are multiplied by $G_0(\zeta), G_1(\zeta)$ and $H_n(\zeta)$ (for all n) due to irregularity of $G_0(\zeta), G_1(\zeta)$ and $H_n(\zeta)$ at the symmetry $z-\text{axis}$. In case of perfect sphere, the stream function solution contains only the terms of order $n = 2$ of the general solution (19). Hence if ψ_i denote the stream function for the internal flow $(r \le a)$, then the stream function solution for the flow field of internal region

$$\psi_i = \Big\{ A_2 r^2 + B_2 r^{-1} + C_2 r^4 + D_2 r + E_2 \sqrt{r} \times K_{3/2}(\lambda r) + F_2 \sqrt{r} I_{3/2}(\lambda r) \Big\} G_2(\zeta). \quad (20)$$

The terms involving $I_{n-\frac{1}{2}}(\lambda r), r^n, r^{n+2}$ create the singularity at infinity except of the term r^2. Therefore the stream function solution for the external flow $(r \ge a)$

$$\psi_e = \Big[A_2' r^2 + B_2' r^{-1} + D_2' r + E_2' \sqrt{r} K_{3/2}(\lambda r) \Big] G_2(\zeta). \quad (21)$$

Since the flow is uniform at infinity that is $\lim_{r\to\infty} \psi_e = \frac{1}{2} r^2 \sin^2\theta$, this implies constant $A_2' = 1$.

Using Eqs. (11), (21) and (20) we obtain the following micro-rotation components υ_ϕ^e and υ_ϕ^i for external and internal flow:

$$\upsilon_\phi^e = \frac{1}{r\sin\theta} \Big\{ \frac{-D_2'}{r} + \Big(\frac{\mu+\kappa}{\kappa} \Big) \lambda^2 E_2' \times \sqrt{r} K_{3/2}(\lambda r) \Big\} G_2(\zeta), \quad (22)$$

and

$$\upsilon_\phi^i = \frac{1}{r\sin\theta} \Big\{ 5C_2 r^2 - \frac{D_2}{r} + \Big(\frac{\mu+\kappa}{\kappa} \Big) \lambda^2 E_2 \times \sqrt{r} K_{3/2}(\lambda r) + \Big(\frac{\mu+\kappa}{\kappa} \Big) \lambda^2 F_2 \sqrt{r} \times I_{3/2}(\lambda r) \Big\} G_2(\zeta). \quad (23)$$

Using Eqs. (2) and (3), we have calculated the pressure distribution for external and internal flow as follows:

$$\mathrm{p}_e = -\Big(\frac{2\mu+\kappa}{\mu} \Big) D_2' \Big(\frac{\cos\theta}{2r^2} \Big), \quad (24)$$

$$\mathrm{p}_i = -\Big(\frac{2\mu+\kappa}{\mu} \Big) \Big(5C_2 r + \frac{D_2}{2r^2} \Big) \cos\theta. \quad (25)$$

Boundary conditions

The boundary conditions those which are physically realistic and mathematically consistent for this proposed problem can be taken as given bellow:

On the outer surface $r = 1$

(i). No-slip condition across the surface implies that

$$\mathrm{v}_\theta^e(r,\theta) = 0, \quad (26)$$

$$\mathrm{v}_\theta^i(r,\theta) = 0. \quad (27)$$

(ii). Zero microrotation components for external and internal flow i.e.

$$\upsilon_\phi^e(r,\theta) = 0, \quad (28)$$

$$\upsilon_\phi^i(r,\theta) = 0. \quad (29)$$

(iii). The normal velocity v_r is continuous at the surface of the sphere and equal to the filtration velocity V with negative sign:

$$\mathrm{v}_r^e(r,\theta) = \mathrm{v}_r^i(r,\theta) = -\mathrm{V}(\theta). \quad (30)$$

(iv). The filtration velocity V is proportional to the difference of the hydrodynamic pressure $\mathrm{p}_e - \mathrm{p}_i$:

$$\mathrm{V}(\theta) = k\big(\mathrm{p}_e(r,\theta) - \mathrm{p}_i(r,\theta) \big), \quad (31)$$

where k is the permeability coefficient > 0.

On the inner surface $r = l = b/a$

(v). Impenetrability at the inner surface requires that

$$\mathrm{v}_r^i(r,\theta) = 0. \quad (32)$$

(vi). No-slip condition at the surface i.e.

$$\mathrm{v}_\theta^i(r,\theta) = 0. \quad (33)$$

(vii). Zero microrotation vector at the inner surface implies we may take

$$\upsilon_{\phi}^{i}(r,\theta)=0. \tag{34}$$

Applying the boundary conditions (26) to (34), we obtain the following linear equations:

$$2-B_2^{'}+D_2^{'}-E_2^{'}\left[\lambda K_{1/2}(\lambda)+K_{3/2}(\lambda)\right]=0, \tag{35}$$

$$2A_2-B_2+4C_2+D_2-E_2\left[\lambda K_{1/2}(\lambda)+K_{3/2}(\lambda)\right]+F_2\left[\lambda I_{1/2}(\lambda)-I_{3/2}(\lambda)\right]=0, \tag{36}$$

$$-D_2^{'}+\left(\frac{\mu+\kappa}{\kappa}\right)\lambda^2E_2^{'}K_{3/2}(\lambda)=0, \tag{37}$$

$$5C_2-D_2+\left(\frac{\mu+\kappa}{\kappa}\right)E_2\lambda^2K_{3/2}(\lambda)+\left(\frac{\mu+\kappa}{\kappa}\right)\times F_2\lambda^2I_{3/2}(\lambda)=0, \tag{38}$$

$$A_2+B_2+C_2+D_2+E_2K_{3/2}(\lambda)+F_2I_{3/2}(\lambda)=1+B_2^{'}+D_2^{'}+E_2^{'}K_{3/2}(\lambda)=k\left(\frac{2\mu+\kappa}{\mu}\right)\times\left(-\frac{D_2^{'}}{2}+5C_2+\frac{D_2}{2}\right). \tag{39}$$

$$A_2l^2+\frac{B_2}{l}+C_2l^4+D_2l+E_2\sqrt{l}K_{3/2}(\lambda l)+F_2\sqrt{l}I_{3/2}(\lambda l)=0, \tag{40}$$

$$2A_2l-\frac{B_2}{l^2}+4C_2l^3+D_2-E_2\sqrt{l}\left[\lambda K_{1/2}(\lambda l)+\frac{1}{l}K_{3/2}(\lambda l)\right]+F_2\sqrt{l}\left[\lambda I_{1/2}(\lambda l)-\frac{1}{l}I_{3/2}(\lambda l)\right], \tag{41}$$

$$5C_2l^2-\frac{D_2}{l}+\left(\frac{\mu+\kappa}{\kappa}\right)E_2\lambda^2\sqrt{l}K_{3/2}(\lambda l)+\left(\frac{\mu+\kappa}{\kappa}\right)F_2\lambda^2\sqrt{l}I_{3/2}(\lambda l)=0, \tag{42}$$

The linear Eqs. (35) to (42) are obtained from boundary conditions (26) to (34) respectively. Value of the all constants $A_2,B_2,C_2,D_2,E_2,F_2,B_2^{'},D_2^{'},E_2^{'}$ are determined by using the above linear equations. Due to very large value of the constants we have not written in this paper except $D_2^{'}$.

4. CALCULATION OF THE DRAG FORCE AND RATE OF FLOW

In order to estimate the drag force due to external flow experienced by the permeable sphere which will be directed along the symmetrical axis, we need to evaluate the integral by Happel and Brenner (1965).

$$D=2\pi a^2\int_0^{\pi}\left(T_{rr}\cos\theta-T_{r\theta}\sin\theta\right)_{r=a}\sin\theta d\theta, \tag{43}$$

where

$$T_{rr}=f(r)\cos\theta,\ T_{r\theta}=g(r)\sin\theta,$$

and

$$f(r)=\frac{U}{a}(2\mu+\kappa)\left\{\left(\frac{3B_2^{'}}{r^4}+\frac{3}{2}\frac{D_2^{'}}{r^2}+\frac{2}{r^3}E_2^{'}\times\left\{\sqrt{r}K_{3/2}(\lambda r)\right\}-\frac{E_2^{'}}{r^2}\left\{\sqrt{r}K_{3/2}(\lambda r)\right\}^{'}\right\},$$

$$g(r)=\frac{U}{2a}(2\mu+\kappa)\left\{\left(\frac{3B_2^{'}}{r^4}+\frac{2}{r^3}E_2^{'}\left\{\sqrt{r}K_{3/2}(\lambda r)\right\}-\frac{E_2^{'}}{r^2}\left\{\sqrt{r}K_{3/2}(\lambda r)\right\}^{'}\right\}.$$

Substituting the values of normal (T_{rr}) and tangential $(T_{r\theta})$ stresses in spherical polar coordinate in Eq. (43) and evaluating the integral, we find that

$$D=2\pi Ua(2\mu+\kappa)D_2^{'}, \tag{44}$$

where $D_2^{'}$ is given in appendix.

The flow rate through the surface is given by Happel and Brenner (1965)

$$Q=\int_{S_1}\mathbf{v.n}\ \mathrm{ds}=-2\pi Ua^2\psi_e(1,0), \tag{45}$$

where S_1 is the front half of the sphere between $0\le\theta\le\pi/2$ and **v.n** the normal component of the velocity.

Hence dimensionless drag experienced by the permeable sphere and flow rate through the permeable sphere is given by $D_N=\dfrac{D}{-6\pi\mu Ua}$ and

$$Q_N=\frac{Q}{-\pi a^2U}=1+B_2^{'}+D_2^{'}+E_2^{'}K_{3/2}(\lambda) \tag{46}$$

respectively.

5. RESULT AND DISCUSSION

At the outset, it is instructive to consider some limiting situations of the drag force as discussed below:

When $\kappa=0$ then micropolar fluid behaves like a Newtonian fluid and in this case from Eq. (44) the calculated drag force comes out

$$D=-\left(6\pi\mu Ua\left(2(1-l)^3\left(4+7l+4l^2\right)+k\left(80+44\times l+44l^2+4l^3+4l^4+4l^5\right)\right)\right)$$

$$/\left(2(1-l)^3\left(4+7l+4l^2\right)\right.$$
$$\left.+k\left(84+39l+39l^2+9l^3+9l^4\right)\right), \qquad (47)$$

which is the drag force for Newtonian fluid past a permeable sphere that contains a solid sphere given by Wolfersdorf (1989).

When $b=0$ i.e. $l=(b/a)=0$ in Eq. (44) then the drag force becomes

$$D=-\left(12a\pi U(1+\lambda)(\kappa+\mu)(\kappa+2\mu)\left(\mu\left(\kappa(15+15\lambda+7\lambda^2+2\lambda^3+e^{2\lambda}(-15+15\lambda-7\lambda^2+2\times\lambda^3)\right)+2\lambda^2\left(1+e^{2\lambda}(-1+\lambda)+\lambda\right)\mu+10k\lambda^2\times\left(1+e^{2\lambda}(-1+\lambda)+\lambda\right)\left(\kappa^2+3\kappa\mu+2\mu^2\right)\right)\right)/\left(2\mu\left(\kappa+2\kappa\lambda+2(1+\lambda)\mu\right)\left(\kappa(15+15\lambda+7\times\lambda^2+2\lambda^3+e^{2\lambda}(-15+15\lambda-7\lambda^2+2\lambda^3)\right)+2\lambda^2\left(1+e^{2\lambda}(-1+\lambda)+\lambda\right)\mu\right)+k\left(\kappa(15+30\lambda+42\lambda^2+69\lambda^3+42\lambda^4e^{2\lambda}(-15-12\lambda^2-25\lambda^3+42\lambda^4)\right)+42\lambda^2(1+\lambda)\left(1+e^{2\lambda}(-1+\lambda)+\lambda\right)\mu\right)\left(\kappa^2+3\kappa\mu+2\mu^2\right)\right), \qquad (48)$$

which is the drag force for micropolar fluid past a permeable sphere with thin surface.

When $b=0$ i.e. $l=b/a=0$ and vertex viscosity $\kappa=0$ in the calculated drag force (44), we get

$$D=-6\pi\mu Ua\left(\frac{1+10k}{1+10.5k}\right), \qquad (49)$$

a well known result for the drag force of Newtonian fluid past a permeable sphere earlier reported by Wolfersdorf (1989). The above result manifests as an important link as we move ahead. Substituting the permeability $k=0$ in Eq. (44) and we find

$$D=-\frac{6\pi Ua(1+\lambda)(\kappa+\mu)(\kappa+2\mu)}{\kappa+2\kappa\lambda+2(1+\lambda)\mu}, \qquad (50)$$

a known result agrees with earlier reported by Ramkisoon and Majumdar (1976) for the drag force past a solid sphere.

Putting vertex viscosity $\kappa=0$ in Eq. (45) we get

$$Q=-\left(3\pi Uka^2(1-l)^3\left(4+7l+4l^2\right)\right)/\left(2(1-l)^3\times\left(4+7l+4l^2\right)+k\left(84+39l+39l^2+9l^3+9l^4\right)\right), \qquad (51)$$

which is the flow rate through the permeable sphere that contains a solid sphere for Newtonian fluid given by Wolfersdorf (1989).

As $b=0$ i.e. $l=(b/a)=0$ when $\kappa=0$ in the rate of flow (45), we obtain

$$Q=-\frac{3}{2}\pi a^2U\left(\frac{k}{1+10.5k}\right), \qquad (52)$$

which is the flow rate through the permeable sphere for Newtonian fluid given by Wolfersdorf (1989).

Drag force at solid sphere:

The drag force due to internal flow experienced by the inner sphere $r=l=(b/a)$ has the value

$$D^*=2\pi(2\mu+\kappa)UD_2. \qquad (53)$$

Substituting vertex viscosity $\kappa=0$ in the calculated drag force (53) we get

$$D^*=-\left(24\pi\mu Ulk\left(6+6l+l^2+l^3+l^4\right)\right)/\left(2(1-l)^3\times\left(4+7l+4l^2\right)+k\left(84+39l+39l^2+9l^3+9l^4\right)\right), \qquad (54)$$

which is the drag force experienced by the inner solid sphere contained in a permeable sphere for the case of Newtonian fluid given by Wolfersdorf (1989).

The parameter $l=\dfrac{b}{a}$ is the separation parameter which represents the extent of closeness between the permeable sphere and solid sphere. Figure 2 presents the effect of separation parameter l on the non-dimensional drag D_N for different value of μ at $\lambda=20,\ \kappa=10,\ k=0.5$. This figure shows that as l increases the drag experienced by the composite sphere increases. Physically it implies that as inner sphere gets bigger the drag acting on the sphere increases. When $l=1$, the

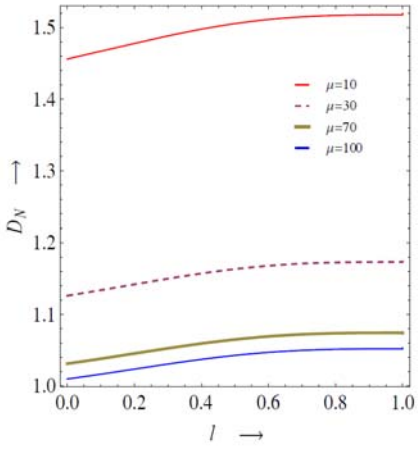

Fig. 2. Variation of drag coefficient D_N verses separation parameter l.

composite sphere geometrically becomes a solid sphere and in this case drag is maximum. Therefore it could be stated explicitly that drag is greater for rigid sphere as compare to permeable sphere.

Figure 3 represents variation of non-dimensional

drag D_N with regard to vertex viscosity κ for various value of μ at $k = 20,\ \lambda = 20,\ l = 0.5$. This graph reveals that as vertex viscosity increases the drag also increases. At $\kappa = 0,$ the micropolar fluid becomes Newtonian. Physically it implies that the drag in Newtonian fluid is less than that of micropolar fluid. The very same observation was made by Gupta and Deo (2013) in the case of axisymmetric creeping flow of micropolar fluid over a sphere coated with a thin fluid film.

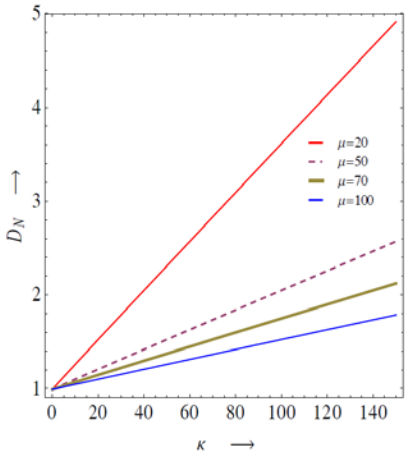

Fig. 3. Dependence of non-dimensional drag D_N on vertex viscosity κ.

Figure 4 depicts graphically the variation in drag coefficient D_N against dynamic viscosity μ for diverse value of l at the fixed values of $\lambda = 20,$ $k = 10$. From Fig. 4 it is clear that as dynamic viscosity increases the drag decreases rapidly. Same

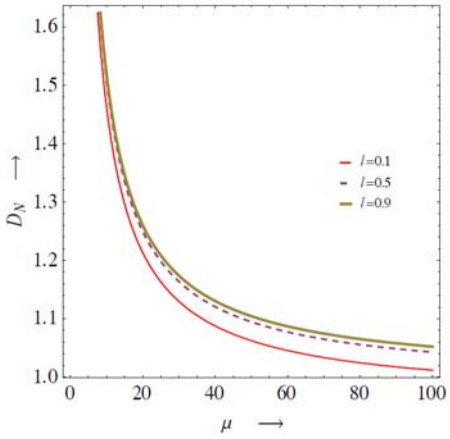

Fig. 4. Variation of non-dimensional drag D_N w.r.t. μ.

observation was also seen in the case of micropolar fluid past a solid sphere. Figure 4 shows that the drag is decreasing sharply when $0 \le \mu \le 40$ and it decreases slowly for $\mu \ge 40$.

The effect of permeability parameter k on non-dimensional drag D_N for different value of l at $\lambda = 20, \kappa = 10, \mu = 10$ is shown in Fig. 5. It is obvious from this figure that, there is measure effect

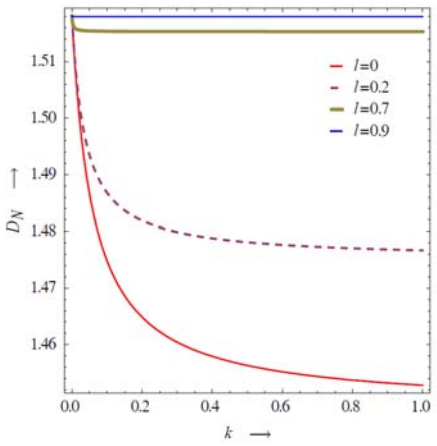

Fig. 5. Variation of non-dimensional drag D_N w.r.t. permeability k .

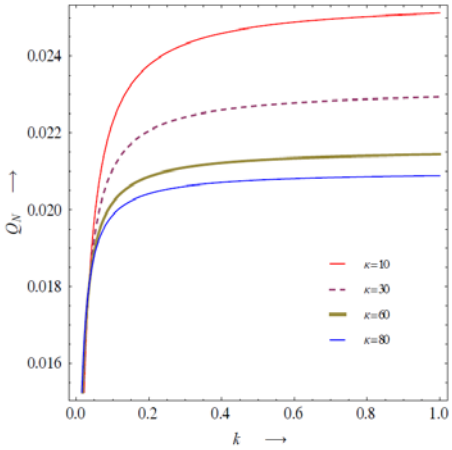

Fig. 6. Variation of non-dimensional flow rate Q_N w.r.t. permeability k .

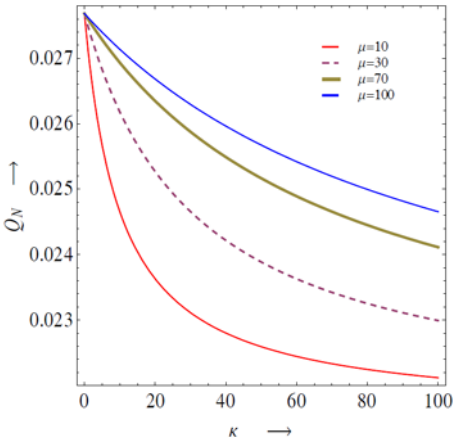

Fig. 7. Variation of non-dimensional flow rate Q_N w.r.t. vertex viscosity κ.

of k on drag. By increasing permeability parameter k the drag is decreasing. When $l = 0$ the composite sphere becomes a hollow permeable sphere and in this case the drag is decreasing rapidly as permeability coefficient k increasing but when $l = 0.9$ the fluid between spheres is very less and the permeable sphere experience greater drag.

Figure 6 exhibits the variation of flow rate Q_N

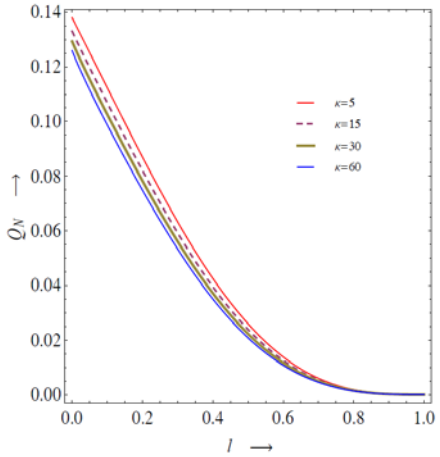

Fig. 8. Variation of non-dimensional flow rate Q_N w.r.t. l .

with respect to permeability parameter k for numerous value of vertex viscosity for the case when $\lambda = 10,\ l = 0.5, \mu = 30.$ It can be observe from the Fig. 6 that by increasing permeability parameter flow rate is increasing rapidly. It is interesting to note that when $k < 0.2$ the flow rate is increasing rapidly and then after it increases gradually.

The graphical representation of non-dimensional flow rate Q_N with respect to vertex viscosity κ is depicted in Fig. 7 for various value of dynamic viscosity μ at fixed values of $\lambda = 10, l = 0.5,$ $k = 10.$ This is obvious from the Fig. 7 that as vertex viscosity increases the rate of flow decreases. Physically it manifests that flow rate is greater in the case of Newtonian than the micropolar fluid, as expected.

Figure 8 shows the variation between non-dimensional flow rate with respect to separation parameter l for different value of vertex viscosity κ . This figure shows that the rate of flow decreases as radius of inner sphere increases. The flow rate becomes almost constant in the interval $0.8 \le l \le 1.$

This work can be extended by using different boundary conditions such as nonhomogeneous boundary condition for microrotation vector, slip boundary condition on the surface of the rigid sphere, stress jump boundary condition for the tangential stress etc. Considering some other viscous fluids like couple stress fluid, Reiner Rivlin fluid, pseudoplastic fluid, instead of micropolar fluid, the same problem can be solved in future.

6. CONCLUSION

In this work an analytical approach is described for steady axisymmetric Stokes flow of micropolar fluid around a permeable sphere with thin surface that contains a solid sphere. The mathematical solutions for the external and internal flow fields are presented in terms of stream function. The drag and the flow rate have been calculated and their variations with respect to different fluid parameter have been plotted. The following observations are made:

(1) It is found that the drag force through the permeable sphere decreases rapidly for very small value of the permeability parameter k and reaches almost constant for very permeable sphere.
(2) Drag coefficient increases when inner sphere gets bigger.
(3) It is observed that drag is greater for the impermeable sphere as compared to the permeable sphere.

It is seen that there is a vast impact of permeability parameter on the rate of flow. As permeability parameter increases the rate of flow also increases sharply.

REFERENCES

Aparna, P. and J. V. R. Murthy (2010). Uniform flow of an incompressible micropolar fluid past a permeable sphere. *International Electronic Engineering Mathematical Society* 8, 1-10.

Aparna, P., J. V. R. Murthy, and G. Nagaraju (2015). Slow steady rotation of a permeable sphere in an incompressible couple stress fluid. *International Journal of Mathematicle Archive* 6(2), 1-9.

Aparna, P., J. V. R. Murthy, and G. Nagaraju (2016). Couple on a rotating permeable sphere in a couple stress fluid. *Ain Shams Engineering Journal.*

Birikh, R. and R. Rudakoh (1982). Slow motion of a permeable sphere in viscous fluid. *Fluid Dynamics* 17(5), 792- 793.

Darcy, H. (1856). *Les Fontaines Publiques. De La Ville De Dijon*. Paris: Victor Dalmont.

Eringen, A. C. (1966). Theory of micropolar fluids. *J. Math. Mech.* Vol. 16, 1-18.

Gupta, B. R. and S. Deo (2013). Axisymmetric creeping flow of micropolar fluid over a sphere coated with a thin fluid film. *Journal of Applied Fluid Mechanics* 6(2), 149-155.

Happel, J. and H. Brenner (1965). *Low Reynolds Number Hydrodynamics.* Englewood Cliffs, NJ: Prentice-Hall.

Happel, J. and H. Brenner (1983). *Low Reynolds Number Hydrodynamics.* Hague: Martinus Nijhoff, Publishers.

Iyengar, T. K. V. and D. Srinivasacharya (1993). Stokes flow of an incompressible micropolar fluid past an approximate sphere. *Int. J. Eng. Sci.* 31, 153-161.

Leonov, A. I. (1962). The slow stationary flow of a viscous fluid about a porous sphere. *Journal of Applied Mathematics and Mechanics* 26, 564-

566.

Madasu, K. P. and M. K. Gurdatta (2015). Steady rotation of micropolar fluid sphere in concentric spherical container. *Procedia Engineering* 127, 469-475.

Masliyah, J. H. and M. Polikar (1980). Terminal velocity of porous spheres. *Can. J. Chem. Eng.* 58, 299-302.

Mishra, V. and B. R. Gupta (2016). Drag on permeable sphere placed in a micropolar fluid with non-zero boundary condition for microrotations. *Journal of Applied Mathematics and Computational Mechanics* 15(3), 103-109.

Mishra, V. and B. R. Gupta (2017). Motion of permeable shell in a spherical container filled with non-Newtonian fluid. *Appl. Math. Mech.*, 38, 1697-1708.

Murthy, J. V. R., N. Srinivasacharyulu, and P. Aparna (2007). Uniform flow of an incompressible couple stress fluid past a permeable sphere. *Bull. Cal. Math. Soc.* 99, 293-304.

Nandakumar, K. and J. H. Masliyah (1982). Laminar flow past a permeable sphere. *The Candadian Journal of Chemical Engineering* 60, 202-211.

Padmavathi, B. S., T. Amarnath, and D. Palaniappan (1995). Stokes flow past a permeable sphere- non axisymmetric case. *Journal of Applied Mathematics and Mechanics* 74, 290-292.

Palaniappan, D., R. Usha, S. D. Nigam, and T. Amarnath (1990). Sphere theorem for Stokes flow. *Mech. Res. Comm.* 17, 173-174.

Ramkisoon, H. and S. R. Majumdar (1976). Drag on an axially symmetric body in the stoke flow of micropolar fluid. *Physics of Fluids* 19(1), 16 -21.

Rao, S. K. L. and P. B. Rao (1970), Slow stationary micropolar fluid past a sphere. J. Eng. Math. 4 209 – 217.

Rao, S. K. L. and T. K. V. Iyengar (1981). The slow stationary flow of incompressible micropolar fluid past a spheroid. *Int. J. Eng. Sci.* 19, 189-220.

Saad, E. I. (2012). Cell model of micropolar fluid past a viscous fluid sphere. *Meccanica* 47, 2055-2068.

Srinivasacharya, D. and I. Rajyalakshmi (2004). Creeping flow of micropolar fluid past a porous sphere. *App. Mathematics and Computation* 153(3), 843-854.

Usha, R. (1995). Creeping flow with concentric permeable spheres in relative motion. *Journal of A pplied Mathematics and Mechanics* 75, 644-646.

Vasudeviah, M. and V. Malathi (1995). Slow viscous flow past a spinning sphere with permeable surface. *Mechanics Research Communications* 22(2), 191-200.

Wolfersdorf, L. V. (1989). Stokes flow past a sphere with permeable surface. *Journal of Applied Mathematics and Mechanics* 69(2), 111-112.

Appendix

$$D_2^{'}=\Big(3\Big(1+\lambda\Big)\big(\kappa+\mu\big)\Big(-2\mu-\Big(k^2\big(1+\lambda\big)\big(\kappa+\mu\big)^2\big(\kappa+2\mu\big)^2\Big(-60e^{\lambda+l\lambda}\sqrt{l}\Big(2+l^3\Big)\kappa\lambda^{5/2}\sqrt{l\lambda}+e^{2\lambda}\Big(15l^5\kappa\big(-1+$$
$$\lambda\big)\lambda+2l^7\big(-1+\lambda\big)\lambda^3\big(\kappa+\mu\big)+20l^3\big(-1+\lambda\big)\lambda^2\big(2\kappa+\mu\big)-20\big(-1+\lambda\big)\lambda^2\big(\kappa+2\mu\big)+l^6\big(-1+\lambda\big)\lambda^2\big(7\kappa+2\mu\big)$$
$$+3l^2\lambda\Big(\kappa\big(5-5\lambda+9\lambda^2+6\lambda^3\big)+\big(-1+\lambda\big)\lambda^2\mu\Big)+5l^4\big(-1+\lambda\big)\Big(\kappa\Big(3+4\lambda^3\Big)+4\lambda^3\mu+l\Big(\kappa\big(15-15\lambda+27\lambda^2+58\lambda^3$$
$$-40\lambda^4\big)-2\lambda^2\big(9-29\lambda+20\lambda^2\big)\mu\big)\Big)+e^{2l\lambda}\Big(-15l^5\kappa\lambda\big(1+\lambda\big)-2l^7\lambda^3\big(1+\lambda\big)\big(\kappa+\mu\big)+20l^3\lambda^2\big(1+\lambda\big)\big(2\kappa+\mu\big)-$$
$$20\lambda^2\big(1+\lambda\big)\big(\kappa+2\mu\big)+l^6\lambda^2\big(1+\lambda\big)\big(7\kappa+2\mu\big)-5l^4\big(1+\lambda\big)\Big(\kappa\Big(-3+4\lambda^3\Big)+4\lambda^3\mu\Big)-3l^2\lambda\Big(\kappa\Big(-5-5\lambda-9\lambda^2+6\lambda^3\Big)$$
$$+6\lambda^2\big(1+\lambda\big)\mu+l\Big(\kappa\Big(-15-15\lambda-27\lambda^2+58\lambda^3+40\lambda^4\Big)+2\lambda^2\big(9+29\lambda+20\lambda^2\big)\mu\Big)\Big)\Big)\Big)\Big)/$$
$$\Big(-12e^{\lambda+l\lambda}\sqrt{l}\kappa\sqrt{\lambda}\sqrt{l\lambda}\Big(2\mu\Big(\kappa^2\big(5+10\lambda-\lambda^2-2\lambda^3+5l^2\lambda^2\big(1+2\lambda\big)+l^5\lambda^2\big(1+2\lambda\big)-5l^3\big(1+2\lambda+\lambda^2+2\lambda^3\big)\Big)+$$
$$\kappa\big(10+10\lambda-3\lambda^2-4\lambda^3+5l^2\lambda^2\big(3+4\lambda\big)+l^5\lambda^2\big(3+4\lambda\big)-5l^3\Big(2+2\lambda+3\lambda^2+4\lambda^3\Big)\Big)\mu+2\big(-1+l\big)^3\Big(1+3l+l^2\Big)\lambda^2\big(1+$$
$$\lambda\big)\mu^2\Big)+k\Big(\kappa^3\big(5+5\lambda+9\lambda^2+19\lambda^3+5l^2\lambda^2\big(1+\lambda\big)+l^5\lambda^2\big(1+\lambda\big)+5l^3\big(-1-\lambda+\lambda^3\big)\Big)+\kappa^2\big(15+15\lambda+46\lambda^2+$$
$$76\lambda^3+20l^2\lambda^2\big(1+\lambda\big)+4l^5\lambda^2\big(1+\lambda\big)+5l^3\big(-3-3\lambda+\lambda^2+4\lambda^3\big)\Big)\mu+5\kappa\big(2+2\lambda+15\lambda^2+19\lambda^3+5l^2\lambda^2\big(1+\lambda\big)+$$
$$l^5\lambda^2\big(1+\lambda\big)\big(1+\lambda\big)+\big(-2-2\lambda+3\lambda^2+5\lambda^3\big)\Big)\mu^2+2\big(19+5l^2+5l^3+l^5\big)\lambda^2\big(1+\lambda\big)\mu^3\Big)\Big)+e^{2l\lambda}\big(2\big(-1+\lambda\big)\mu\Big(\kappa^3\big(15+45\lambda+$$

$$37\lambda^2+16\lambda^3+4\lambda^4+2l^6\lambda^3(1+2\lambda)^2-l^5\lambda^2\left(7+35\lambda+47\lambda^2+10\lambda^3\right)+l^4\lambda\left(15+80\lambda+106\lambda^2+7\lambda^3-10\lambda^4\right)-$$
$$l\lambda\left(45+140\lambda+121\lambda^2+46\lambda^3+8\lambda^4\right)+l^2\lambda\left(-30-80\lambda-34\lambda^2+17\lambda^3+10\lambda^4\right)+l^3\left(-15-75\lambda-70\lambda^2+66\lambda^3+57\lambda^4\right.$$
$$\left.+10\lambda^5\right)\Big)+2\kappa^2\left(30+75\lambda+60\lambda^2+28\lambda^3+8\lambda^4+l^6\lambda^3\left(5+16\lambda+12\lambda^2\right)-l^5\lambda^2\left(15+59\lambda+61\lambda^2+15\lambda^3\right)+l^4\lambda\left(30+\right.\right.$$
$$120\lambda+109\lambda^2+2\lambda^3-15\lambda^4\Big)-l\lambda\left(60+150\lambda+136\lambda^2+59\lambda^3+12\lambda^4\right)+l^2\lambda\left(-30-60\lambda-31\lambda^2+22\lambda^3+15\lambda^4\right)+$$
$$3l^3\left(-10-35\lambda-15\lambda^2+28\lambda^3+24\lambda^4+5\lambda^5\right)\Big)\mu+(-1+l)\kappa(1+\lambda)\Big(8l^5\lambda^3(2+3\lambda)-3l^4\lambda^2\left(12+19\lambda+2\lambda^2\right)+l^3\lambda\left(60+\right.$$
$$69\lambda-40\lambda^2-36\lambda^3\Big)-4\left(15+15\lambda+9\lambda^2+5\lambda^3\right)+l^2\left(-60+114\lambda^2+47\lambda^3-6\lambda^4\right)+3l\left(-20+23\lambda^2+18\lambda^3+8\lambda^4\right)\Big)\mu^2+$$

$$2(-1+l)^3\left(4+7l+4l^2\right)\lambda^2(1+\lambda)^2(-1+l\lambda)\mu^3\Big)-3k\Big(\kappa^4\left(5+10\lambda+14\lambda^2+23\lambda^3+14\lambda^4+15l^2\lambda^5\right)-9l^5\lambda^2(1+\lambda)^2+$$
$$3l^6\lambda^3(1+\lambda)^2+10l^4\lambda\left(1+2\lambda+\lambda^2+\lambda^3+\lambda^4\right)-5l^3\left(1+2\lambda+\lambda^2+4\lambda^3+4\lambda^4\right)-l\lambda\left(10+20\lambda+28\lambda^2+61\lambda^3+28\lambda^4\right)\Big)+$$
$$\kappa^3\left(25+50\lambda+84\lambda^2+143\lambda^3+84\lambda^4-39l^5\lambda^2(1+\lambda)^2+15l^6\lambda^3(1+\lambda)^2+15l^2\lambda^4(2+5\lambda)+10l^4\lambda\left(4+8\lambda+5\lambda^2+6\lambda^3+\right.\right.$$
$$5\lambda^4\Big)-5l^3\left(5+10\lambda+9\lambda^2+22\lambda^3+18\lambda^4\right)-5l\lambda\left(8+16\lambda+34\lambda^2+63\lambda^3+28\lambda^4\right)\Big)\mu+\kappa^2\left(-57l^5\lambda^2(1+\lambda)^2+\right.$$
$$27l^6\lambda^3(1+\lambda)^2+15l^2\lambda^3\left(1+8\lambda+9\lambda^2\right)+10l^4\lambda\left(5+10\lambda+9\lambda^2+13\lambda^3+9\lambda^4\right)-10l^3\left(4+8\lambda+11\lambda^2+21\lambda^3+14\lambda^4\right)+$$
$$2\left(20+40\lambda+91\lambda^2+162\lambda^3+91\lambda^4\right)-l\lambda\left(50+115\lambda+372\lambda^2+589\lambda^3+252\lambda^4\right)\Big)\mu^2+\kappa\left(-33l^5\lambda^2(1+\lambda)^2+\right.$$
$$21l^6\lambda^3(1+\lambda)^2+15l^2\lambda^3\left(3+10\lambda+7\lambda^2\right)+10l^4\lambda\left(2+4\lambda+7\lambda^2+12\lambda^3+7\lambda^4\right)-10l^3\left(2+4\lambda+9\lambda^2+16\lambda^3+9\lambda^4\right)$$
$$+4\left(5+10\lambda+42\lambda^2+79\lambda^3+42\lambda^4\right)-l\lambda\left(20+85\lambda+346\lambda^2+477\lambda^3+196\lambda^4\right)\Big)\mu^3+2\left(-28+15l+10l^3+\right.$$
$$\left.3l^5\right)\lambda^2(1+\lambda)^2(-1+l\lambda)\mu^4\Big)\Big)+e^{2\lambda}\Big(-2(-1+l)\mu\Big(\kappa^3\left(15+15\lambda-23\lambda^2+12\lambda^3-4\lambda^4+l^5\lambda^2\left(-7+7\lambda+37\lambda^2-10\lambda^3\right)\right.\right.$$

$$+l^4\lambda\left(-15+20\lambda+94\lambda^2-17\lambda^3-10\lambda^4\right)+l\lambda\left(45+40\lambda-79\lambda^2+38\lambda^3-8\lambda^4\right)+l^2\lambda\left(30+40\lambda-46\lambda^2-7\lambda^3+10\lambda^4\right)$$
$$+l^6\left(-2\lambda^3+8\lambda^5\right)+l^3\left(-15+15\lambda+110\lambda^2+14\lambda^3-47\lambda^4+10\lambda^5\right)\Big)+2\kappa^2\left(30+15\lambda-30\lambda^2+18\lambda^3-8\lambda^4+l^6\lambda^3\left(-5+12\lambda^2\right)\right.$$
$$+l^5\lambda^2\left(-15+13\lambda+41\lambda^2-15\lambda^3\right)+l^4\lambda\left(-30+30\lambda+91\lambda^2-22\lambda^3-15\lambda^4\right)+l^2\lambda\left(30-49\lambda^2-2\lambda^3+15\lambda^4\right)+l\left(60\lambda-64\lambda^3\right.$$
$$+43\lambda^4-12\lambda^5\Big)+l^3\left(-30+15\lambda+105\lambda^2-4\lambda^3-52\lambda^4+15\lambda^5\right)\Big)\mu+(-1+l)\kappa\left(8l^5\lambda^3\left(-2+3\lambda^2\right)+l^4\lambda^2\left(-36+13\lambda+\right.\right.$$
$$53\lambda^2-6\lambda^3\Big)+l^3\lambda\left(-60+9\lambda+111\lambda^2+16\lambda^3-36\lambda^4\right)+4\left(-15+6\lambda^2-6\lambda^3+5\lambda^4\right)-l^2\left(60+60\lambda-114\lambda^2-79\lambda^3\right.$$
$$+51\lambda^4+6\lambda^5\Big)+l\left(-60-60\lambda+69\lambda^2+17\lambda^3-38\lambda^4+24\lambda^5\right)\Big)\mu^2+2(-1+l)^3\left(4+7l+4l^2\right)\lambda^2(1+l\lambda)\left(-1+\lambda^2\right)\mu^3\Big)$$
$$+k\Big(\kappa^4\left(15+12\lambda^2+25\lambda^3-42\lambda^4-4l^7\lambda^4+l^6\lambda^3\left(-23+9\lambda^2\right)+3l^5\lambda^2\left(-19+9\lambda^2\right)+10l^4\lambda\left(-6+3\lambda^2-\lambda^3+3\lambda^4\right)+\right.$$
$$5l^3\left(-3+3\lambda^2-4\lambda^3+12\lambda^4\right)+l\left(60\lambda+78\lambda^3+95\lambda^5-84\lambda^5\right)+l^2\left(30\lambda^2+54\lambda^4+45\lambda^5\right)\Big)+\kappa^3\left(75+102\lambda^2+125\lambda^3\right.$$
$$-252\lambda^4-16l^7\lambda^4+9l^5\lambda^2\left(-23+13\lambda^2\right)+l^6\lambda^3\left(-91+45\lambda^2\right)+9l^2\lambda^2\left(10+24\lambda^2+25\lambda^3\right)+10l^4\lambda\left(-21+9\lambda^2-4\lambda^3\right.$$
$$+15\lambda^4\Big)+5l^3\left(-15+3\lambda^2-14\lambda^3+54\lambda^4\right)+l\left(210\lambda+396\lambda^3+425\lambda^4-420\lambda^5\right)\Big)\mu+\kappa^2\left(120+306\lambda^2+200\lambda^3-\right.$$
$$546\lambda^4-20l^7\lambda^4+3l^5\lambda^2\left(-77+57\lambda^2\right)+l^6\lambda^3\left(-121+81\lambda^2\right)+15l^2\lambda^2\left(4-3\lambda+18\lambda^2+27\lambda^3\right)+l\lambda\left(210-45\lambda+\right.$$
$$726\lambda^2+655\lambda^3-756\lambda^4\Big)+10l^4\lambda\left(-21+3\lambda^2-5\lambda^3+27\lambda^4\right)+10l^3\left(-12-9\lambda^2-7\lambda^3+42\lambda^4\right)\Big)\mu^2+\kappa\Big(60+384\lambda^2$$
$$+100\lambda^3-504\lambda^4-8l^7\lambda^4+99l^5\lambda^2\left(-1+\lambda^2\right)+9l^2\lambda^3\left(-15+12\lambda+35\lambda^2\right)+l^6\lambda^3\left(-71+63\lambda^2\right)+l\lambda\left(60-135\lambda+\right.$$
$$576\lambda^2+415\lambda^3-588\lambda^4\Big)+10l^4\lambda\left(-6-9\lambda^2-2\lambda^3+21\lambda^4\right)+10l^3\left(-6-15\lambda^2-2\lambda^3+27\lambda^4\right)\Big)\mu^3+6\left(-28+15l+\right.$$
$$\left.\left.\left.10l^3+3l^5\right)\lambda^2(1+l\lambda)\left(-1+\lambda^2\right)\mu^4\right)\right)\Big)\Big)\Big)/\left(2\mu\left(\kappa+2\kappa\lambda+2(1+\lambda)\mu\right)+k(1+\lambda)\left(\kappa^2+3\kappa\mu+2\mu^2\right)\right).$$

.